

Authored by a member of



<sup>a</sup>Institute of Biomaterials and Biomedical Engineering, University of Toronto, Toronto, Ontario, Canada; <sup>b</sup>Translational Biology and Engineering Program, Ted Rogers Centre for Heart Research, Toronto, Ontario, Canada; <sup>c</sup>Department of Physiology, University of Toronto, Toronto, Ontario, Canada; <sup>d</sup>Department of Surgery, Division of Plastic and Reconstructive Surgery, University of Toronto, Toronto, Ontario, Canada; <sup>e</sup>Departments of Surgery and Surgical Oncology, University Health Network, Toronto, Ontario, Canada; <sup>f</sup>Faculty of Dentistry, University of Toronto, Toronto, Ontario, Canada

Correspondence: J. Paul Santerre, Ph.D., Institute of Biomaterials and Biomedical Engineering, University of Toronto, 661 University Ave., 14th Floor, Room 1435, Toronto, Ontario, Canada M5G 1M1. Telephone: +1 (416) 946-8158; e-mail: paul.santerre@utoronto.ca

Received June 7, 2018; accepted for publication August 3, 2018; first published September 30, 2018.

<http://dx.doi.org/10.1002/ctm.18-0127>

This is an open access article under the terms of the Creative Commons Attribution-NonCommercial-NoDerivs License, which permits use and distribution in any medium, provided the original work is properly cited, the use is non-commercial and no modifications or adaptations are made.

## Limited Endothelial Plasticity of Mesenchymal Stem Cells Revealed by Quantitative Phenotypic Comparisons to Representative Endothelial Cell Controls

JEREMY A. ANTONYSHYN <sup>a,b</sup> MEGHAN J. MCFADDEN <sup>a,b</sup> ANTHONY O. GRAMOLINI <sup>b,c</sup>  
STEFAN O.P. HOFER <sup>d,e</sup> J. PAUL SANTERRE <sup>a,b,f</sup>

**Key Words.** Mesenchymal stromal cells • Adult stem cells • Endothelial cells • Cell differentiation • Cell plasticity

### ABSTRACT

Considerable effort has been directed toward deriving endothelial cells (ECs) from adipose-derived mesenchymal stem cells (ASCs) since 2004, when it was first suggested that ECs and adipocytes share a common progenitor. While the capacity of ASCs to express endothelial markers has been repeatedly demonstrated, none constitute conclusive evidence of an endothelial phenotype as all reported markers have been detected in other, non-endothelial cell types. In this study, quantitative phenotypic comparisons to representative EC controls were used to determine the extent of endothelial differentiation being achieved with ASCs. ASCs were harvested from human subcutaneous abdominal white adipose tissue, and their endothelial differentiation was induced using well-established biochemical stimuli. Reverse transcription quantitative real-time polymerase chain reaction and parallel reaction monitoring mass spectrometry were used to quantify their expression of endothelial genes and corresponding proteins, respectively. Flow cytometry was used to quantitatively assess their uptake of acetylated low-density lipoprotein (AcLDL). Human umbilical vein, coronary artery, and dermal microvascular ECs were used as positive controls to reflect the phenotypic heterogeneity between ECs derived from different vascular beds. Biochemically conditioned ASCs were found to upregulate their expression of endothelial genes and proteins, as well as AcLDL uptake, but their abundance remained orders of magnitude lower than that observed in the EC controls despite their global proteomic heterogeneity. The findings of this investigation demonstrate the strikingly limited extent of endothelial differentiation being achieved with ASCs using well-established biochemical stimuli, and underscore the importance of quantitative phenotypic comparisons to representative primary cell controls in studies of differentiation. *STEM CELLS TRANSLATIONAL MEDICINE* 2019;8:35–45

### SIGNIFICANCE STATEMENT

Adipose-derived mesenchymal stem cells have been pursued as endothelial cell substitutes for the vascularization of tissue-engineered constructs since their capacity to express endothelial markers was first reported in 2004. This is the first study to emphasize the strikingly limited extent of endothelial differentiation being achieved with these cells, suggesting that they may not be the suitable endothelial cell substitutes that have been advocated for tissue engineering applications. Perhaps more importantly, this study may serve as a cautionary finding to anyone exploring the plasticity of a cell, where quantitative phenotypic comparisons to representative primary cell controls may be scarce. The findings may also serve as the impetus for exploring alternative sources of endothelial cells for regenerative medicine applications.

### INTRODUCTION

The vascularization of tissue-engineered constructs is generally considered to be the most significant technical challenge facing their clinical translation [1]. Constructs exceeding the

100–200  $\mu\text{m}$  diffusion limit of oxygen and nutrients through tissues require a network of blood vessels to facilitate their perfusion and, thereby, sustained survival and function [2]. The poor rate of physiological neovascularization has

prompted the development of alternative strategies to expedite their perfusion, such as the *in vitro* incorporation of vascular networks that are amenable to microsurgical or physiological anastomosis to the host vasculature [1, 3]. However, its fabrication from primary endothelial cells (ECs) is hampered by the low prevalence of these cells in tissues [4], and the identification of a suitable alternative remains a formidable challenge [2, 3].

A suitable source of ECs for tissue engineering applications will be autologous to preclude immunogenic concerns, readily accessible to minimize the donor site morbidity associated with its procurement, and accruable in sufficient quantities for the *in vitro* vascularization of constructs that are of a clinically relevant size. Accordingly, considerable effort has been directed toward deriving ECs from adipose-derived mesenchymal stem cells (ASCs) since Planat-Benard et al. first suggested that ECs and adipocytes share a common progenitor in 2004 [5]. The abilities of various biochemical [6, 7], biomechanical [8, 9], and substrate [10, 11] stimuli to promote the endothelial differentiation of ASCs have been investigated. These studies have repeatedly demonstrated the capacity of ASCs to express molecular endothelial markers, as well as their ability to perform endothelial functions such as uptake acetylated low-density lipoprotein (AcLDL), secrete nitric oxide, and self-assemble into vascular-like networks [6–11]. This has led many to believe that they have successfully derived EC substitutes, with which they have attempted the *in vitro* vascularization of tissue-engineered constructs [12].

The expression of molecular and functional endothelial markers by conditioned ASCs does not, however, constitute conclusive evidence of their successful differentiation. There are no known markers that are constitutively, nor exclusively, expressed by ECs; that is, the expression of endothelial markers is variable between ECs derived from different vascular beds, and all have been identified in other, non-endothelial cell types [13, 14]. The absence of uniformly expressed markers with specificity to the endothelial lineage presents a significant challenge to the assessment of an endothelial phenotype. In fact, it has previously misled others to mistake omental mesothelial cells for microvascular ECs [15], monocytes for endothelial progenitor cells [16], and platelets for circulating ECs [17]. Accordingly, a critical evaluation of the phenotype for endothelially differentiated ASCs is warranted prior to their implementation in tissue-engineered constructs.

The purpose of this investigation was to critically evaluate the endothelial plasticity of ASCs. Quantitative phenotypic comparisons to several representative EC controls were used to determine the extent of endothelial differentiation being achieved with ASCs using well-established biochemical stimuli.

## MATERIALS AND METHODS

### Cell Isolation and Culture

Subcutaneous abdominal white adipose tissue was obtained with informed consent from patients undergoing reconstructive breast surgery at the University Health Network (Toronto, ON, Canada). This procedure was approved by the institutional

research ethics board (#13-6437-CE). Unless indicated otherwise, all other materials were obtained from Sigma-Aldrich (St. Louis, MO, <http://www.sigmaaldrich.com>).

ASCs were isolated from the stromal vascular fraction of adipose tissue using an adapted protocol [18]. Briefly, adipose tissue was rinsed with phosphate-buffered saline (PBS), finely minced and enzymatically digested for 60 minutes at 37°C under agitation using collagenase type II (2 mg/ml) in Kreb's Ringer bicarbonate buffer supplemented with 3 mM glucose, 25 mM 4-(2-hydroxyethyl)-1-piperazineethanesulfonic acid, and 20 mg/ml bovine serum albumin. The digest was centrifuged at 1,200g for 5 minutes at 25°C, and the resulting cell pellet was rinsed with PBS and subjected to another round of enzymatic digestion for 15 minutes at 37°C using 2.5 mg/ml trypsin. The cells were then resuspended in an erythrocyte-lysing buffer (0.154 M ammonium chloride, 10 mM potassium bicarbonate, and 0.1 mM ethylenediaminetetraacetic acid in sterile deionized water), and agitated for 10 minutes at 25°C to facilitate erythrocyte lysis. The sample was resuspended in Dulbecco's Modified Eagle Medium and Ham's F-12 nutrient mixture (DMEM:F12; supplemented with 10% (v/v) fetal bovine serum, 100 U/ml penicillin, and 0.1 mg/ml streptomycin) and filtered through a 100 µm sieve. The resulting filtrate was defined as the stromal vascular fraction and was immediately depleted of CD45<sup>+</sup> leukocytes and CD31<sup>+</sup> ECs using Dynabeads (Invitrogen, Carlsbad, CA, <http://www.invitrogen.com>). The CD45<sup>-</sup>CD31<sup>-</sup> stromal vascular cells were plated onto tissue-culture polystyrene (TCPS) at a concentration of 25,000 cells/cm<sup>2</sup> and maintained under humidity at 37°C, 5% CO<sub>2</sub> in DMEM:F12 media. After 24 hours, the cells were rinsed with PBS to remove non-adherent cells and particulate, and the media replenished. The TCPS-adherent CD45<sup>-</sup>CD31<sup>-</sup> stromal vascular cells were defined as ASCs [8, 9].

Human umbilical vein ECs (HUVECs; Lonza, Walkersville, MD, <https://www.lonza.com>), human coronary artery ECs (HCAECs; Lonza) and human dermal microvascular ECs (HDMVECs; Lonza and PromoCell, Heidelberg, Baden-Württemberg, Germany, <https://www.promocell.com>) were obtained commercially and maintained under humidity at 37°C, 5% CO<sub>2</sub> in EC growth medium-2 (EGM2; Lonza). For all cells, media was exchanged three times a week and cells were passaged at 75%–90% confluence using TrypLE Express (Gibco, Carlsbad, CA, <http://www.thermofisher.com>). Light microscopy was used to assess their morphology and confluence (Leica DMIL, Wetzlar, Hesse, Germany, <https://www.leica-microsystems.com>). Cells were counted using a hemocytometer, and dead cells were excluded on the basis of trypan blue uptake. Cells from passages two to five were used for subsequent experiments.

### Immunophenotyping

The immunophenotype of ASCs was assessed by flow cytometry in accordance with previously established guidelines [19]. ASCs were stained with Live/Dead Fixable Aqua (Invitrogen) and Fc receptors were blocked using Human TruStain FcX (BioLegend, San Diego, CA, <https://www.biolegend.com>). Cells were then stained for 30 minutes at 4°C, protected from light, with combinations of the following fluorophore-conjugated mouse anti-human monoclonal antibodies: CD45-APC/Cy7 (BioLegend), CD31-Alexa Fluor 488 (BioLegend), CD105-APC (BioLegend), CD44-Brilliant Blue 515 (Becton, Dickinson and Company, Franklin Lakes, NJ, [www.bd.com](http://www.bd.com)), CD13-Brilliant

Violet 650 (Becton, Dickinson and Company), CD29-PE (BioLegend), CD73-PE/Cy7 (BioLegend), and CD90-PE Dazzle 594 (BioLegend). Stained cells were fixed in 2% (v/v) formaldehyde in PBS for 30 minutes at 4°C. Compensation was achieved using the AbC Anti-Mouse Bead Kit and the ArC Amine Reactive Compensation Bead Kit (Life Technologies, Carlsbad, CA, <https://www.thermofisher.com/>). Cells were analyzed using a BD LSR II, BD LSRFortessa or BD LSRFortessa X-20 flow cytometer (Becton, Dickinson and Company), and data were analyzed using FlowJo software version 10.1 (Tree Star, Ashland, OR, <https://www.flowjo.com>).

### Fibroblastoid Colony-Forming Units

A fibroblastoid colony-forming unit (CFU-F) assay was adapted from Pochampally [20]. Briefly, ASCs were seeded onto TCPS at a concentration of 2 cells/cm<sup>2</sup> in DMEM:F12 media and maintained under humidity at 37°C, 5% CO<sub>2</sub>. After 14 days, the media were aspirated, cells rinsed with PBS and stained with 3% (v/v) crystal violet in methanol for 10 minutes at 25°C. The number of colonies ≥ 2 mm in diameter was divided by the total number of cells seeded to determine the frequency of CFU-F.

### Adipogenic, Osteogenic, and Chondrogenic Differentiation

The multipotency of ASCs was characterized in accordance with previously established guidelines [19]. Specifically, the adipogenic, osteogenic, and chondrogenic differentiation of ASCs was induced using StemPro Differentiation Kits (Gibco), and their differentiation along each of these lineages was evaluated by Oil Red O, von Kossa, and Alcian Blue staining, respectively.

### Endothelial Differentiation

The endothelial differentiation of ASCs was induced using EGM2, as commonly performed [7, 9–11]. Specifically, ASCs were seeded onto TCPS at a density of 5 × 10<sup>3</sup> cells/cm<sup>2</sup> in DMEM:F12 medium and maintained under humidity at 37°C, 5% CO<sub>2</sub>. After 24 hours, the media were aspirated, cells rinsed with PBS, and the media exchanged with EGM2. Media were replenished three times a week for 14 days, after which their endothelial phenotype was evaluated. Unconditioned ASCs—that is, ASCs maintained in DMEM:F12 medium for 14 days—served as negative controls. The positive EC control comprised HUVECs, HCAECs, and HDMVECs cultured in EGM2 for 14 days, which were evaluated separately but statistically presented as a single population in order to reflect the inherent variability between ECs derived from different vascular beds [13, 14]. All cells were passaged at 75%–90% confluence.

### Gene Expression

Total ribonucleic acid (RNA) was isolated from cells using Trizol (Invitrogen). Its concentration and ratio of absorbance at 260–280 nm ( $A_{260/280}$ ) was evaluated using a spectrophotometer (NanoDrop 2000, Thermo Fisher Scientific, Waltham, MA, <https://www.thermofisher.com>), and only samples with an  $A_{260/280} \geq 1.80$  were considered free from protein contamination and used for downstream applications. The integrity of isolated RNA was assessed using the Agilent RNA 6000 Nano Kit (Agilent, Santa Clara, CA, <http://www.agilent.com>), and a ratio of 28–18 s ribosomal RNA subunits of approximately 2.0 suggested that RNA did not undergo degradation using this procedure (data not shown). A total of 1 µg of RNA from the above-mentioned preparation

was immediately reverse transcribed into complementary deoxyribonucleic acid (cDNA) using the High Capacity cDNA Reverse Transcription Kit (Applied Biosystems, Foster City, CA, <http://www.appliedbiosystems.com>).

Reverse transcription quantitative real-time polymerase chain reaction (RT-qPCR) was performed on a CFX384 Touch Real-Time PCR Detection System (Bio-Rad, Hercules, CA, <http://www.bio-rad.com>). All experiments utilized three technical replicates for each biological sample, and included no reverse transcription controls. Amplification was achieved and detected using the SsoAdvanced Universal SYBR Green Supermix (Bio-Rad), with each reaction comprising 10 ng template cDNA and 450 nM of both forward and reverse primers in a total volume of 10 µl. The reaction consisted of the following steps: polymerase activation (95°C, 30 seconds); 35 cycles of cDNA denaturation (95°C, 10 seconds) followed by primer annealing and extension (61.6°C, 30 seconds, fluorescence measurement); and, finally, cDNA denaturation (95°C, 30 seconds) followed by a melting curve program (65°C–95°C, heating 0.5°C per 5 seconds, continuous fluorescence measurements). A primer annealing and extension temperature of 61.6°C was found to be optimal for the efficient and specific amplification by all pairs of primers using a thermal gradient ranging from 55°C to 65°C (data not shown).

The nucleotide sequences of the primers designed to amplify genes of interest are delineated in Table 1, and they were validated in line with previously established guidelines [21]. Briefly, primer specificity was supported by both melt curve analyses, with each PCR product exhibiting a single melting temperature, as well as amplicon size quantification using the Agilent DNA 1000 Kit (Agilent), in which each reaction yielded a single product of the expected length. PCR efficiency for each pair of primers was assessed across a ≥5-point, 10- or 5-fold dilution series of template cDNA starting from 100 ng, and the linear dynamic range was defined by an efficiency of 90%–105% and a squared Pearson's correlation coefficient ( $r^2$ ) ≥ 0.98. The results of these primer validation studies are summarized in Table 1.

Relative gene expression was quantified as described by Pfaffl [22]. Briefly, expression of the gene of interest was normalized to that of glyceraldehyde-3-phosphate dehydrogenase (GAPDH) and reported relative to an ASC control, based on the corresponding PCR efficiencies and quantification cycles ( $C_q$ ). Statistical analyses were performed on log<sub>2</sub>-transformed fold change values.

### Global and Targeted Proteomic Analyses

Sample preparation was carried out using an adapted protocol [23]. Briefly, cells derived from a 90% confluent 75 cm<sup>2</sup> TCPS flask were resuspended in a solubilization buffer (50% (v/v) 2,2,2-trifluoroethanol in PBS supplemented with 100 mM ammonium bicarbonate), sonicated and incubated at 60°C for 2 hours to extract proteins. Samples were then reduced with 5 mM dithiothreitol for 30 minutes at 55°C, and alkylated with 15 mM iodoacetamide for 30 minutes at 25°C in the dark. Following 1:5 dilution with 100 mM ammonium bicarbonate, and addition of 2 mM calcium chloride, proteins were digested overnight at 37°C with 5 µg of mass spectrometry (MS)-grade Trypsin-Lys C mix (Promega, Madison, WI, <http://www.promega.com>), and an additional 2 hours with 2 µg of MS-grade Trypsin-Lys C mix. Formic acid was added to a final concentration of 5% (v/v) to quench the digestion, after which the samples were centrifuged at 10,000g for 10 minutes at 25°C to remove aggregates.

**Table 1.** Design and validation of primers employed in quantitative real-time polymerase chain reaction (PCR) experiments. Nucleotide sequences of the primers are delineated, as well as the efficiency, correlation and linear dynamic range of their reactions. Empirically determined melting temperatures and lengths of their corresponding products are also reported.

Gene	Primer nucleotide sequence		PCR efficiency			PCR product	
	Forward primer 5' → 3'	Reverse primer 3' → 5'	Efficiency %	Correlation $r^2$	Range ng cDNA	$T_m$ °C	Length bp
GAPDH	CTCCTGTTCGACAGTCAGCC	CCTCAGTTGCCTAAACCAGC	101.6	.997	0.0001–100	86.5	106
CD31	GTCCTGATGCCGTGGAAAG	AATACTGGACGGGACGAGG	104.1	.997	0.001–10	84.0	178
VE-cadherin	CTTACCCAGACCAAGTACACA	TGGTCTCGCAAAGTGTTAA	96.7	.997	0.001–10	87.0	164
CD34	GACCCTGATTGCACTGGTCA	CTCTTCCGACCCGCTTCTG	96.8	.986	0.032–20	87.0	119
VEGFR2	GAGGGGAAGTGAAGACAGGC	CGATCCATTCGAGAACC GG	100.6	.996	0.0064–20	84.5	143
vWF	TTGACGGGGAGGTGAATGTG	GCACCAGGACTTCGTCTGTA	103.2	.999	0.001–10	87.5	158
eNOS	CTGTGAGACCTTCTGTGTGGG	TCAACGACGGTCCAGACTAGG	99.2	.991	0.0064–20	90.0	142
CD146	TGGGCGCTGTCTCTATTC	GGGCAGACATTCTCGCTTG	100.1	.998	0.0064–20	86.0	105

Abbreviations: cDNA, complementary deoxyribonucleic acid; eNOS, endothelial nitric oxide synthase; GAPDH, glyceraldehyde-3-phosphate dehydrogenase; PCR, polymerase chain reaction;  $r$ , Pearson's correlation coefficient;  $T_m$ , melting temperature; bp, base pairs; VE-cadherin, vascular endothelial-cadherin; VEGFR2, vascular endothelial growth factor receptor-2; vWF, von Willebrand Factor.

Tryptic peptides were de-salted using OMIX C18 solid-phase extraction tips (Agilent). Samples were dried by vacuum centrifugation and reconstituted in 30  $\mu$ l 5% (v/v) formic acid in high-performance liquid chromatography (HPLC)-grade water.

Tryptic peptides were analyzed by reversed-phase liquid chromatography—tandem MS (LC-MS/MS) on an Easy-nLC 1200 (Thermo Fisher Scientific) coupled to a Q Exactive Plus mass spectrometer (Thermo Fisher Scientific). Tryptic peptides were loaded onto an in-house packed reversed-phase 10-cm, 75  $\mu$ m i.d. column (Reprosil-Pur Basic C18, 3  $\mu$ m, 100  $\text{\AA}$ ; Dr. Maisch HPLC, Ammerbuch, Baden-Württemberg, Germany, <http://www.dr-maisch.com>), and separated using a 3-hour acetonitrile linear gradient (2%–35% (v/v) in HPLC-grade water) at 250 nl/minute. The eluent was introduced directly into the mass spectrometer using a Nanospray Flex Ion Source (Thermo Fisher Scientific). All experiments utilized two technical replicates for each biological sample. For global proteomic analyses, spectra were collected using a top 10 data-dependent acquisition (DDA) method with settings of resolution ( $R$ ) = 70,000 at 200  $m/z$  for one full MS1 scan from 400 to 1,500  $m/z$  for a maximum injection time of 100 ms, followed by 10 data-dependent MS2 scans for a maximum injection time of 55 ms at  $R$  = 17,500 with 30 seconds dynamic exclusion, and excluding 1+ and >6+ precursor ion charge states. Normalized high energy collision-induced dissociated energy (NCE) was set at 28. RAW files were searched against the UniProt human proteome database (updated to July 24, 2017) using the Andromeda algorithm [24] within MaxQuant software version 1.6.0.1 (Max Planck Institute of Biochemistry, Planegg, Bavaria, Germany, <http://www.biochem.mpg.de/en>). Cysteine carbamidomethylation was set as a fixed modification, and methionine oxidation, N-terminal acetylation, and asparagine or glutamine deamidation were selected as variable modifications. The false discovery rate (FDR) was set to 1% using a reversed-target decoy database. Raw files and search results are available from MASSIVE with accession code: MSV000082318. Hierarchical clustering of proteins that were identified in  $\geq 2$  biological replicates in at least one group was conducted using the Perseus 1.6.1.2 software package (Max Planck Institute of Biochemistry), based on label-free quantification (LFQ) values [25] that were scaled to a 1–1,000 interval per protein. One-way analysis of variance was used to identify proteins that were differentially expressed between groups ( $p < .05$ ).

Targeted proteomic analyses were used to quantify the relative abundance of seven proteins of interest [26]. Using spectral matches from the global DDA analyses, two proteotypic peptides were selected for each protein, avoiding those with missed cleavage sites or variable modifications when possible (Table 2). LC-MS/MS was carried out in parallel reaction monitoring mode following high energy collision-induced dissociation of 14 precursor ions corresponding to the target peptides. Raw files and the transition list are available from PASSSEL with accession code: PASS01229. Extracted ion chromatograms (XICs) for up to nine fragment ions (0.05  $m/z$  isolation width) per precursor ion were generated using XCalibur 4.1 Qual Browser software (Thermo Fisher Scientific). Peaks were selected based on similar retention time between samples, and comprising at least the most abundant base peak (i.e., most intense fragment ion). The area under the curve (AUC) of the XICs for the two proteotypic peptides for each protein were added together and normalized to that of GAPDH, and reported relative to an ASC control. An XIC AUC of 10 was assigned to samples for which the target protein was not detected to facilitate reporting of fold change. The proteotypic peptides and corresponding fragment ions used to generate the XICs for proteins of interest are delineated in Table 2. Statistical analyses were performed on  $\log_2$ -transformed fold change values.

### AcLDL Uptake

The uptake of AcLDL by ASCs and ECs was assessed using an adapted protocol [6, 8, 9]. Specifically, cells were incubated with 10  $\mu$ g/ml Alexa Fluor 488–conjugated AcLDL (Life Technologies) for 4 hours under humidity at 37°C, 5% CO<sub>2</sub>, after which they were fixed in 2% (v/v) formaldehyde in PBS for 30 minutes at 4°C in the dark. Cells were analyzed using a BD LSR II flow cytometer (Becton, Dickinson and Company), and data were analyzed using FlowJo software version 10.1 (Tree Star). The median fluorescence intensity (MFI) of the stained cells was divided by the MFI of the corresponding unstained cells to normalize for their autofluorescence and was reported relative to an ASC control. Statistical analyses were performed on  $\log_2$ -transformed fold change values.

### Statistical Analyses

Statistical analyses were performed using Prism 7 (GraphPad Software, La Jolla, CA, <https://www.graphpad.com>). Two-tailed paired

**Table 2.** Precursor ions and their corresponding fragment ions assessed in parallel reaction monitoring liquid chromatography tandem-mass spectrometry assays. Two proteotypic peptides (i.e., precursor ions) per protein of interest were selected to undergo collision-induced dissociation, and up to nine fragment ions per peptide were used to generate extracted ion chromatograms. The amino acid sequence, charge state and mass-to-charge ratio of each proteotypic peptide is delineated, as well as their corresponding b- and y-fragment ions.

Protein	Precursor ion			Fragment ion
	Amino acid sequence	z	m/z	
GAPDH	GALQNIIPASTGAAK	+2	706.3988	y6, y8, y9, y10, y11
	VIHDNFGIVEGLMTTVHAITATQK	+3	865.7915	y7, b7, y8, b8, y9, y11, b11, y12
CD31	DQNFVILEFPVEEQDR	+2	989.4813	y7, y8, y9, y10, y11, y12, y13, y14
	STESYFIPEVR	+2	664.3301	y4, y5, y6, y7, y8, y9
VE-cadherin	YEIVVEAR	+2	489.7664	y4, y5, y6, y7
	VHFLPVVISDNGMPSR	+3	589.9785	y6, y7, y8, y9, y10, y11, y12, y13
VEGFR2	FLSTLTIDGVTR	+2	661.8694	y4, y5, y6, y7, y8, y9
	LGQPPLPIHVGELPTPVC(+57) <sup>a</sup> K	+3	684.7152	y4, y5, y6, y7, y8, y9, y10
vWF	IGWPNAPILIQDFETLPR	+3	694.0457	y4, y5, y6, y7, y8, y9, y10, y11, y12
	VTVPPIGIGDR	+2	587.335	y5, y6, y7, y8, y9, y10
eNOS	VEDPPAPTEPVAVEQLEK	+2	974.4991	y6, y7, y8, y9, y10, y11, y12, y13, y14
	GGC(+57) <sup>a</sup> PADWAWIVPPISGSLTPVFHQEMVNYFLSPAFR	+3	1349.6622	y11, y12, y13, y14, y15, y16, y17, y18
CD146	VHIQSSQTVESGLYTLQSIK	+3	806.7673	y5, y6, y7, y8, y9, y10, y11, y12
	SELVVEVK	+2	451.7633	y4, y5, y6, y7

<sup>a</sup> Cysteine residues are carbamidomethylated, conferring a 57 Da mass increase.

Abbreviations: eNOS, endothelial nitric oxide synthase; GAPDH, glyceraldehyde-3-phosphate dehydrogenase; m/z, mass-to-charge ratio; VE-cadherin, vascular endothelial-cadherin; VEGFR2, vascular endothelial growth factor receptor-2; vWF, von Willebrand Factor; z, charge.

*t* tests were used to compare conditioned and control ASCs, blocking for donors. ASCs were compared to the EC controls using one-way analysis of variance, with Tukey's post hoc test for multiple comparisons. The Pearson's correlation coefficients between GAPDH-normalized  $C_q$  values and GAPDH-normalized XIC AUC values were used to evaluate the relationship between mRNA and protein abundance for each marker of interest, and only samples for which both data sets were collected and detected were included in the analyses.  $p < .05$  was accepted as statistically significant. Values are represented as mean  $\pm$  SD.

## RESULTS

### Isolation and Characterization of ASCs

ASCs were isolated from the stromal vascular fraction of enzymatically digested human subcutaneous abdominal white adipose tissue. Immunomagnetic beads were used to deplete the stromal vascular fraction of CD45<sup>+</sup> leukocytes and CD31<sup>+</sup> ECs to prevent their contamination of ASC cultures from confounding subsequent evaluations of the endothelial plasticity of ASCs [8, 9]. ASCs were defined as the TCPS-adherent CD45<sup>-</sup>CD31<sup>-</sup> stromal vascular cells [8, 9]. They exhibited a spindle-shaped fibroblast-like morphology (Fig. 1A;  $N = 3$ ) and were capable of clonal expansion ( $33.1 \pm 3.5\%$  CFU-F;  $N = 3$ ). They were negative for the pan-hematopoietic marker CD45 ( $0.4 \pm 0.3\%$ ) and endothelial marker CD31 ( $0.1 \pm 0.0\%$ ), and expressed characteristic stromal markers CD13 ( $99.8 \pm 0.1\%$ ), CD44 ( $99.9 \pm 0.1\%$ ), CD105 ( $88.9 \pm 4.3\%$ ), CD29 ( $96.7 \pm 5.5\%$ ), CD90 ( $97.2 \pm 4.8\%$ ), and CD73 ( $99.9 \pm 0.1\%$ ; Supporting Information Fig. S1;  $N = 3$ ) [19]. The multipotency of the ASCs was demonstrated by their differentiation along the adipogenic (Fig. 1B), osteogenic (Fig. 1C), and chondrogenic (Fig. 1D) lineages ( $N = 3$ ) [19].

### Evaluation of the Endothelial Plasticity of ASCs

The endothelial differentiation of ASCs was induced using EGM2, as commonly performed [7, 9–11]. This media is

supplemented with factors implicated in the differentiation and survival of ECs, including vascular endothelial growth factor and basic fibroblast growth factor [27]. The endothelial phenotype of ASCs was evaluated after 14 days of conditioning, and was compared to that of HUVECs, HCAECs, and HDMVECs to better reflect the phenotypic heterogeneity between ECs derived from different vascular beds [13, 14]. These EC controls were cultured under the same conditions as the ASCs to prevent differences in their microenvironment from confounding subsequent evaluations of their endothelial phenotype [28].

The global proteomes of the EC controls were evaluated by LC-MS/MS to assess their ability to represent a broad endothelial phenotype. A total of 4,462 proteins were identified, and 3,745 were further analyzed on the basis of being identified in  $\geq 2$  biological replicates corresponding to at least one vascular bed (Fig. 2;  $N = 3$ ). With exception to HDMVECs from one donor, unsupervised hierarchical clustering of their global protein expression profiles resulted in the grouping of HUVECs, HCAECs, and HDMVECs (Fig. 2C), indicating that pervasive proteomic patterns distinguish ECs derived from different vascular beds despite their *in vitro* culture under identical conditions. Of the 3,745 proteins that were analyzed, 520 were found to be differentially expressed between the groups ( $p < .05$ ) and their hierarchical clustering revealed patterns that distinguished macrovascular ECs (i.e., HUVECs and HCAECs) from microvascular ECs (i.e., HDMVECs), as well as venous ECs (i.e., HUVECs) from arterial ECs (i.e., HCAECs; Fig. 2D). Together, these findings indicate that the variability in endothelial phenotypes between HUVECs, HCAECs, and HDMVECs is greater than the donor-to-donor variability between ECs derived from the same vascular bed, supporting the ability of this assortment of positive controls to better represent an endothelial phenotype than ECs derived from a single vascular bed. Accordingly, endothelially conditioned ASCs were compared to this combination of positive controls for all subsequent experiments.

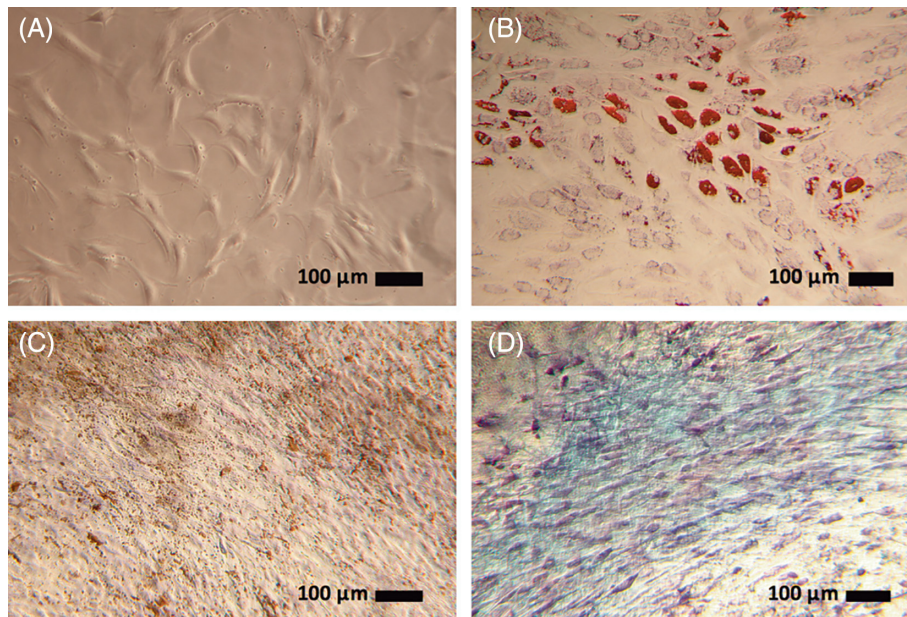


**Figure 1.** Morphology and multipotency of adipose-derived mesenchymal stem cells (ASCs). **(A):** Representative phase-contrast photomicrograph of ASCs adhered to tissue-culture polystyrene ( $N = 3$ ), obtained with an objective magnification of  $\times 4$ . **(B):** Oil Red O staining of ASCs cultured in adipogenic differentiation medium for 14 days ( $N = 3$ ). Red staining is indicative of triglycerides and lipids. **(C):** von Kossa staining of ASCs cultured in osteogenic differentiation medium for 28 days ( $N = 3$ ). Brown staining is indicative of mineralization. **(D):** Alcian Blue staining of ASCs cultured in chondrogenic differentiation medium for 28 days ( $N = 3$ ). Blue staining is indicative of proteoglycans. **(B–D):** Positive staining was not observed in unstimulated ASC controls (data not shown). Representative photomicrographs were taken by bright-field light microscopy using an objective magnification of  $\times 4$ .

### Molecular Endothelial Phenotype of Conditioned ASCs

The differentiation of ASCs along the endothelial lineage will manifest itself at the molecular level as alterations in their transcriptome and proteome. Although there are no known markers that are exclusively, nor constitutively, expressed by ECs, there are several that are commonly expressed together and, accordingly, are often used to evaluate an endothelial phenotype [13, 14]. These include CD31, vascular endothelial (VE)-cadherin, CD34, vascular endothelial growth factor receptor-2 (VEGFR2), von Willebrand Factor (vWF), endothelial nitric oxide synthase (eNOS), and CD146. RT-qPCR and parallel reaction monitoring LC-MS/MS were used to quantify the abundance of their corresponding mRNA transcripts and proteins, respectively, to determine the extent of endothelial differentiation achieved with the ASCs relative to the EC controls. ASCs conditioned in EGM2 were found to generally upregulate their expression of endothelial genes ( $N = 6$ ), albeit to levels significantly lower than that observed in the EC controls ( $N = 3$ ; Fig. 3A). Similarly, the abundance of endothelial proteins was elevated in conditioned ASCs ( $N = 4$ ), but was lower than that observed in the EC controls ( $N = 3$ ; Fig. 3B). There was a significant correlation between mRNA and protein abundance for each endothelial marker evaluated, with exception to CD34 which was not detected at the protein level (Fig. 3C, 3D).

### Functional Endothelial Phenotype of Conditioned ASCs

The uptake of AcLDL is generally considered a function unique to ECs and macrophages, and its uptake by conditioned ASCs is often cited as evidence of their successful differentiation [6, 8, 9]. ASCs were found to basally uptake AcLDL, and their conditioning in EGM2 increased both the proportion of cells that take it up as well

as the quantity of its uptake (Fig. 4; Supporting Information Fig. S2;  $N = 3$ ). While there was no statistically significant difference in the proportion of cells that uptake AcLDL between conditioned ASCs and the EC controls (Fig. 4B), the quantity of AcLDL uptake by conditioned ASCs was significantly lower than that by the EC controls (Fig. 4C; Supporting Information Fig. S2).

Perhaps one of the best defining features of ECs, however, is their anatomical presentation, where they form a confluent monolayer lining the luminal surface of the vasculature [14]. Fortunately, this property is visibly conserved by ECs *in vitro*; specifically, ECs proliferate to yield a confluent monolayer of a cobblestone-like morphology, with their growth arrested upon homotypic cell contact [14]. In contrast to the HUVECs, HCAECs, and HDMVECs that exhibited this characteristic endothelial behavior and morphology, conditioned ASCs retained a spindle-shaped, fibroblast-like morphology similar to that observed in the unconditioned ASC controls and failed to exhibit contact-mediated growth inhibition (Fig. 5;  $N = 3$ ).

### DISCUSSION

ASCs have been pursued as EC substitutes for the vascularization of tissue-engineered constructs since Planat-Benard et al. first suggested that ECs and adipocytes share a common progenitor in 2004 [5]. Although their capacity to express molecular and functional endothelial markers has been repeatedly demonstrated [6–11], this is the first study to implement quantitative phenotypic comparisons to representative EC controls in order to demonstrate the strikingly limited extent of endothelial differentiation being achieved with ASCs using well-established biochemical stimuli. The abundance of endothelial

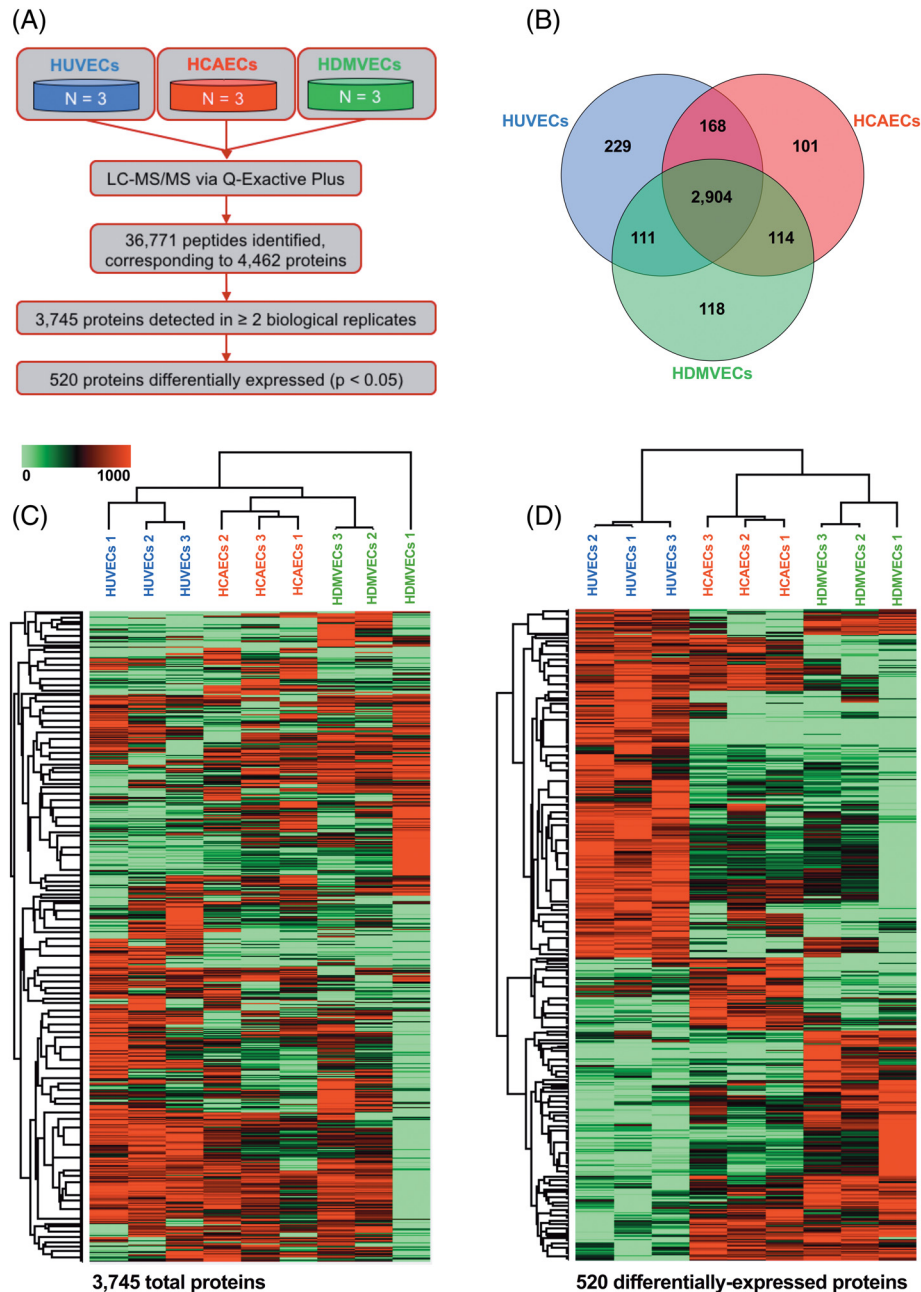


**Figure 2.** Protein expression profiles of endothelial cells (ECs) derived from different vascular beds. **(A):** Workflow of the global proteomic analysis of ECs. Human umbilical vein ECs (HUVECs;  $N = 3$ ), human coronary artery ECs (HCAECs;  $N = 3$ ), and human dermal microvascular ECs (HDMVECs;  $N = 3$ ) were cultured in vitro under identical conditions, lysed, and their tryptic peptides assessed by liquid chromatography tandem-mass spectrometry. **(B):** Venn diagram depicting the number of proteins shared between the different types of ECs, based on their detection in  $\geq 2$  biological replicates per group. **(C):** Heat map depicting the hierarchical clustering of the global proteomes of ECs, based on label-free quantification (LFQ) values of proteins detected in  $\geq 2$  biological replicates in at least one group. **(D):** Heat map depicting the hierarchical clustering of proteins determined to be differentially expressed between the different types of ECs by one-way analysis of variance ( $p < .05$ ). **(C, D):** Scale bar represents LFQ values scaled to a 0–1,000 interval per protein. Abbreviations: HCAECs, human coronary artery endothelial cells; HDMVECs, human dermal microvascular endothelial cells; HUVECs, human umbilical vein endothelial cells; LC-MS/MS, liquid chromatography tandem-mass spectrometry.

mRNA, protein, and AcLDL uptake in biochemically conditioned ASCs, albeit elevated, remained orders of magnitude lower than that observed by the three distinct EC controls. Furthermore, conditioned ASCs failed to exhibit a cobblestone-like morphology and contact-mediated growth inhibition, both of which are hallmarks of an EC [14]. Importantly, the expression of both molecular and functional endothelial markers by conditioned

ASCs was markedly lower than that by the EC controls despite their global proteomic heterogeneity, supporting the limited plasticity of ASCs toward the endothelial lineage of any specialization and tissue localization.

The failure of previous investigations to detect the limited endothelial plasticity of ASCs may be largely attributed to their use of qualitative assays and their omission of representative

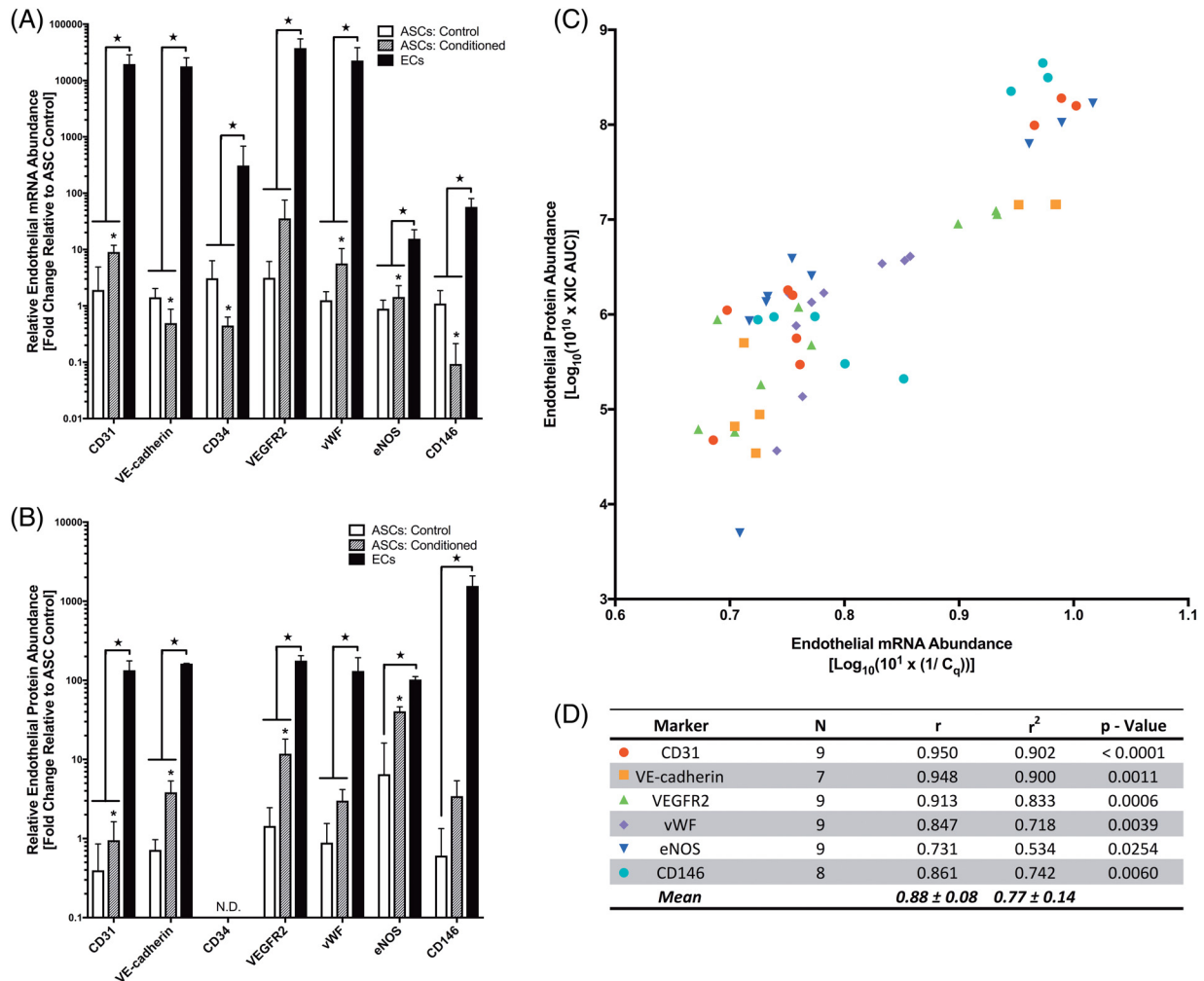


**Figure 3.** Expression of molecular endothelial markers by adipose-derived mesenchymal stem cells (ASCs). ASCs and the three distinct endothelial cell (EC) controls were cultured in EC growth medium-2 (EGM2) for 14 days, after which their expression of endothelial genes and proteins were assessed by reverse transcription quantitative real-time polymerase chain reaction and parallel reaction monitoring liquid chromatography tandem-mass spectrometry, respectively. **(A):** Expression of endothelial genes by unconditioned ASCs ( $N = 6$ ), conditioned ASCs ( $N = 4$ ), and the EC controls ( $N = 3$ ). **(B):** Expression of endothelial proteins by unconditioned ASCs ( $N = 4$ ), conditioned ASCs ( $N = 4$ ), and the EC controls ( $N = 3$ ). **(A, B):** Expression was normalized to glyceraldehyde-3-phosphate dehydrogenase (GAPDH) and is reported relative to an ASC control. Values represent mean  $\pm$  SD; \* $p < .05$  relative to unconditioned ASC controls; and  $\star p < .05$ . **(C):** Scatter plot depicting the correlation between the abundance of messenger ribonucleic acid (mRNA) and protein for each endothelial marker, and **(D):** a table delineating the corresponding Pearson's correlation coefficients and  $p$ -values. Values represent mean  $\pm$  SD. Abbreviations: ASCs, adipose-derived mesenchymal stem cells;  $C_q$ , quantification cycle; ECs, endothelial cells; eNOS, endothelial nitric oxide synthase; N.D., not detected;  $r$ , Pearson's correlation coefficient; VE-cadherin, vascular endothelial-cadherin; VEGFR2, vascular endothelial growth factor receptor-2; vWF, von Willebrand Factor; XIC AUC, extracted ion chromatogram area under the curve.

primary cell controls in evaluating an endothelial phenotype. The expression of endothelial genes by ASCs has often been evaluated by end-point PCR [6, 8], and that of proteins by Western blots [8, 9], immunofluorescence microscopy [6–8, 10, 11], and flow cytometry [7, 9]. Similarly, AcLDL uptake has predominantly been assessed by immunofluorescence microscopy [6, 8, 9]. Although these techniques are effective in demonstrating the induction of endothelial markers by stimulated ASCs, their mere expression is insufficient to support an endothelial phenotype due to their lack of specificity to the endothelial lineage [13, 14]. Accordingly, quantitative assays are needed to determine the extent of their expression relative to EC controls to more thoroughly evaluate the endothelial phenotype of conditioned ASCs. Of the studies that employed quantitative phenotypic assays, namely RT-qPCR [7, 9–11, 29],

only Zhang et al. and Shojaei et al. compared the expression of endothelial genes by conditioned ASCs to that by a positive control [9, 29]. While both studies found their expression to be lower in conditioned ASCs than in HUVECs, the extent of the discrepancies was obscured by the means used to present the data. This absence of direct quantitative phenotypic comparisons between “differentiated” ASCs and ECs in the literature has impeded an accurate evaluation of the extent of endothelial differentiation being achieved.

Defining the successful endothelial differentiation of ASCs is not only made challenging by the absence of EC-specific markers, but it is further complicated by the heterogeneity between ECs derived from different vascular beds [13, 14]. Chi et al. evaluated the transcriptomes of 52 ECs derived from 14 different vascular beds and found gene expression patterns

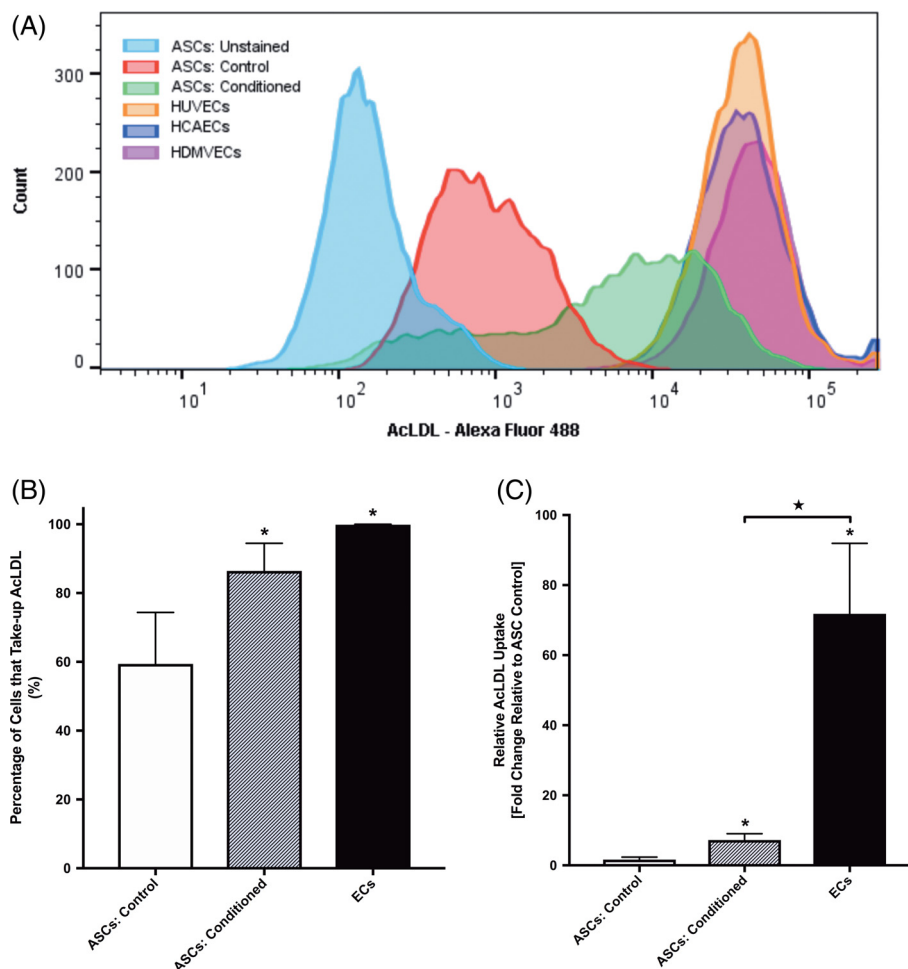


**Figure 4.** Uptake of acetylated low-density lipoprotein (AcLDL) by adipose-derived mesenchymal stem cells (ASCs). Unconditioned ASC controls ( $N = 3$ ), ASCs conditioned in endothelial cell (EC) growth medium-2 (EGM2) for 14 days ( $N = 3$ ), and the three distinct EC controls ( $N = 3$ ) were incubated with Alexa Fluor 488-conjugated AcLDL for 4 hours, after which their uptake of the molecule was assessed by flow cytometry. **(A)**: Representative histogram of AcLDL uptake by the different cells. **(B)**: Percentage of cells that stained positively for AcLDL uptake. **(C)**: Relative AcLDL uptake by the cells. Uptake was normalized to a negative control, and is reported relative to an ASC control. **(B, C)**: Values represent mean  $\pm$  SD; \* $p < .05$  relative to unconditioned ASC controls; and  $\star p < .05$ . Abbreviations: AcLDL, acetylated low-density lipoprotein; ASCs, adipose-derived mesenchymal stem cells; ECs, endothelial cells; HCAECs, human coronary artery endothelial cells; HDMVECs, human dermal microvascular endothelial cells; HUVECs, human umbilical vein endothelial cells.

that distinguish macrovascular ECs from microvascular ECs and arterial ECs from venous ECs, despite their *in vitro* culture under identical conditions [30]. These pervasive differences in expression of molecular endothelial markers preclude a single positive control from being representative of an endothelial phenotype. Accordingly, HUVECs, HCAECs, and HDMVECs were used as positive controls in this investigation to better reflect the phenotypic heterogeneity between ECs derived from different vascular beds. Similar to the major subpopulations of ECs identified by Chi et al. [30], patterns in their protein expression profiles distinguished macrovascular HUVECs and HCAECs from microvascular HDMVECs, as well as arterial HCAECs from venous HUVECs, supporting the capacity of these EC controls to encompass a broad endothelial phenotype.

Quantitative phenotypic comparisons to this combination of EC controls were used to facilitate an accurate assessment of the extent of endothelial differentiation being achieved with ASCs. RT-qPCR and parallel reaction monitoring LC-MS/MS were used to quantify the relative abundance of endothelial mRNA and their corresponding proteins, respectively. In

accordance with the central dogma of biology that describes the process by which DNA is sequentially transcribed into mRNA and then translated into proteins to confer a phenotype to a cell, there was a significant correlation between mRNA and protein abundance for each endothelial marker evaluated, with exception to CD34 which was not detected at the protein level. The failure of this investigation to detect CD34 is not surprising, as both ASCs and ECs have been reported to down-regulate the expression of CD34 *in vitro* [31, 32]. Interestingly, greater quantities of VE-cadherin and CD146 were detected in conditioned ASCs than in ASC controls despite a lower abundance of their corresponding mRNA transcripts. These discrepancies may be attributed to post-transcriptional mechanisms regulating protein abundance, as transcript levels are known to only partially predict protein abundances; in fact, it has been proposed that transcription may act like a switch, with post-transcriptional, translational, and degradative mechanisms being ultimately responsible for modulating protein abundance [33]. Nevertheless, the relatively strong correlation between mRNA and protein abundance (average  $r^2 = .77$  in

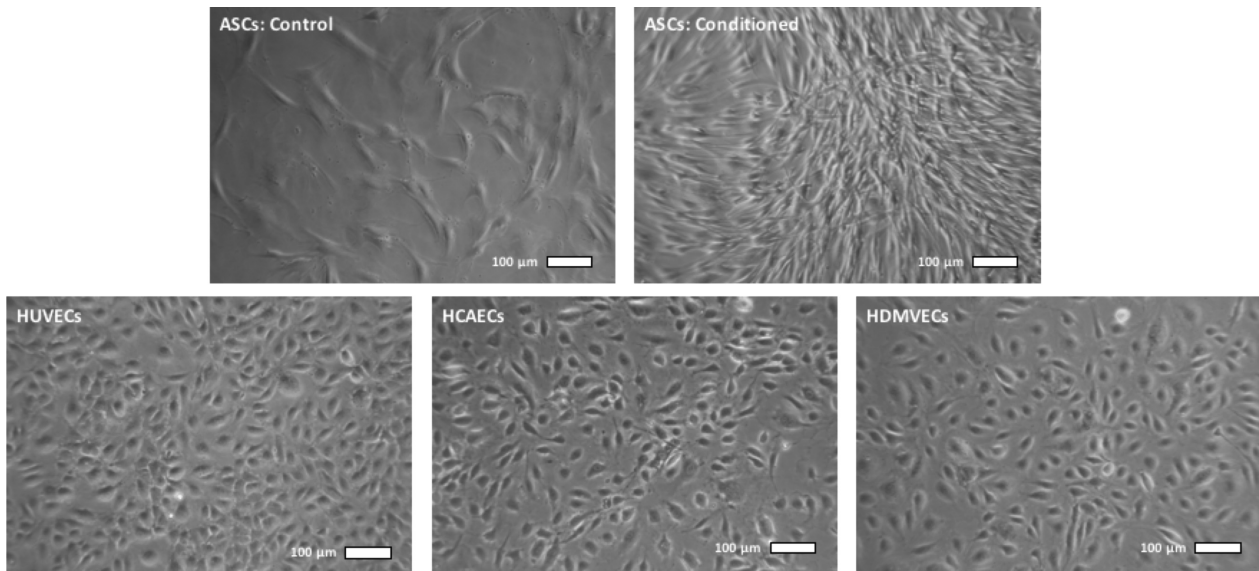


**Figure 5.** Morphology of adipose-derived mesenchymal stem cells and endothelial cells cultured in endothelial cell growth medium 2 (EGM2) for 14 days ( $N = 3$ ). Representative photomicrographs were obtained with phase-contrast light microscopy using an objective magnification of  $\times 10$ . Abbreviations: ASCs, adipose-derived mesenchymal stem cells; HCAECs, human coronary artery endothelial cells; HDMVECs, human dermal microvascular endothelial cells; HUVECs, human umbilical vein endothelial cells.

this study vs.  $r^2 \sim .40$  reported in the literature [33]) supports the accuracy of the RT-qPCR and parallel reaction monitoring LC-MS/MS assays employed in this investigation. In addition to the quantitative evaluation of endothelial protein expression, this was the first study to use flow cytometry in a quantitative capacity to compare the relative uptake of AcLDL by conditioned ASCs and ECs. Together, the findings of this investigation demonstrated the markedly limited transcriptomic, proteomic, and, ultimately, functional endothelial traits being induced in ASCs with their culture in EGM2.

The endothelial differentiation of ASCs was induced using EGM2 because it is the most commonly employed stimulus reported in the literature [7, 9–11]. Compared to conditioning ASCs with EGM2 alone, however, subjecting them to shear stress has been shown to further upregulate vWF by approximately 25% [9]; their culture on nanograted substrates has been found to nearly double the abundance of CD31, VE-cadherin and vWF transcripts [10]; and, their three-dimensional culture has been shown to potentiate their upregulation of CD31 and VEGFR2 approximately 7- and 13-fold, respectively [11]. The magnitudes of these upregulations are negligible, however, when compared to their level of expression in ECs, where CD31 was found by RT-qPCR in this investigation to be expressed approximately 19,600 times greater than in ASCs; VE-cadherin, 17,800 times; vWF, 22,600 times; and VEGFR2, 37,600 times. This minimal expression of endothelial markers by conditioned ASCs suggests an inherent, epigenetic limitation on their endothelial plasticity, such as DNA methylation and histone modifications that constrain their ability to express endothelial genes and, thereby, an endothelial phenotype [34]. In fact, Culmes et al. demonstrated that treating ASCs with an epigenetic-modifying drug that reduced the extent of their DNA methylation also increased their capacity to express endothelial markers [34], supporting the presence of inherent, epigenetic limitations on the endothelial plasticity of ASCs.

## CONCLUSION

This is the first investigation to critically evaluate the endothelial plasticity of ASCs. Quantitative phenotypic comparisons to representative EC controls were used to demonstrate the strikingly limited extent of endothelial differentiation being achieved with ASCs using well-established biochemical stimuli. The expression of transcriptomic, proteomic, and functional endothelial markers by conditioned ASCs was shown to be significantly lower than that observed in ECs despite their global proteomic heterogeneity, suggesting that they may not be suitable EC substitutes for the vascularization of tissue-engineered constructs.

## ACKNOWLEDGMENTS

The authors thank Kate Butler, Anne O'Neill, and Toni Zhong for their contributions to the provision of human tissue for this research, and Xiaoqing Zhang for assisting with the characterization of the ASCs. This work was funded by the Canadian Institutes for Health Research (MOP 230762), as well as seed grants to A.O. Gramolini and J.P. Santerre from the Ted Rogers Centre for Heart Research. J.A. Antonyshyn was supported by Ontario Graduate Scholarships, a Canada Graduate Scholarship from the Natural Sciences and Engineering Research Council of Canada, and a Ted Rogers Centre for Heart Research Education Fund.

## AUTHOR CONTRIBUTIONS

J.A.A.: conception and design, collection and/or assembly of data, data analysis and interpretation, manuscript writing, final approval of manuscript; M.J.M.: collection and/or assembly of data, final approval of manuscript; A.O.G.: provision of study material or patients, final approval of manuscript; S.O.P.H.:

provision of study material or patients, final approval of manuscript; J.P.S.: provision of study material or patients, financial support, final approval of manuscript.

#### DISCLOSURE OF POTENTIAL CONFLICTS OF INTEREST

The authors indicated no potential conflicts of interest.

#### REFERENCES

- 1 Rouwkema J, Khademhosseini A. Vascularization and angiogenesis in tissue engineering: Beyond creating static networks. *Trends Biotechnol* 2016;34:733–745.
- 2 Jain RK, Au P, Tam J et al. Engineering vascularized tissue. *Nat Biotechnol* 2005;23:821–823.
- 3 Rouwkema J, Rivron NC, van Blitterswijk CA. Vascularization in tissue engineering. *Trends Biotechnol* 2008;26:434–441.
- 4 van Beijnum JR, Rousch M, Castermans K et al. Isolation of endothelial cells from fresh tissues. *Nat Protoc* 2008;3:1085–1091.
- 5 Planat-Benard V, Silvestre JS, Cousin B et al. Plasticity of human adipose lineage cells toward endothelial cells: Physiological and therapeutic perspectives. *Circulation* 2004;109:656–663.
- 6 Cao Y, Sun Z, Liao L et al. Human adipose tissue-derived stem cells differentiate into endothelial cells in vitro and improve postnatal neovascularization in vivo. *Biochem Biophys Res Commun* 2005;332:370–379.
- 7 Khan S, Villalobos MA, Choron RL et al. Fibroblast growth factor and vascular endothelial growth factor play a critical role in endotheliogenesis from human adipose-derived stem cells. *J Vasc Surg* 2017;65:1483–1492.
- 8 Fischer LJ, McIlhenny S, Tulenko T et al. Endothelial differentiation of adipose-derived stem cells: Effects of endothelial cell growth supplement and shear force. *J Surg Res* 2009;152:157–166.
- 9 Zhang P, Moudgill N, Hager E et al. Endothelial differentiation of adipose-derived stem cells from elderly patients with cardiovascular disease. *Stem Cells Dev* 2011;20:977–988.
- 10 Shi Z, Neoh KG, Kang ET et al. Enhanced endothelial differentiation of adipose-derived stem cells by substrate nanotopography. *J Tissue Eng Regen Med* 2014;8:50–58.
- 11 Qiu X, Zhang Y, Zhao X et al. Enhancement of endothelial differentiation of adipose derived mesenchymal stem cells by a three-dimensional culture system of microwell. *Biomaterials* 2015;53:600–608.
- 12 Auxenfans C, Lequeux C, Perrusel E et al. Adipose-derived stem cells (ASCs) as a source of endothelial cells in the reconstruction of endothelialized skin equivalents. *J Tissue Eng Regen Med* 2012;6:512–518.
- 13 Garlanda C, Dejana E. Heterogeneity of endothelial cells: Specific markers. *Arterioscler Thromb Vasc Biol* 1997;17:1193–1202.
- 14 Aird WC. Phenotypic heterogeneity of the endothelium: I. Structure, function, and mechanisms. *Circ Res* 2007;100:158–173.
- 15 Visser MJT, van Bockel JH, van Muijen GNP et al. Cells derived from omental fat tissue and used for seeding vascular prostheses are not endothelial in origin. A study on the origin of epitheloid cells derived from omentum. *J Vasc Surg* 1991;13:373–381.
- 16 Rehman J, Li J, Orschell CM et al. Peripheral blood “endothelial progenitor cells” are derived from monocyte/macrophages and secrete angiogenic growth factors. *Circulation* 2003;107:1164–1169.
- 17 Strijbos MH, Kraan J, den Bakker MA et al. Cells meeting our immunophenotypic criteria of endothelial cells are large platelets. *Cytometry B Clin Cytom* 2007;72B:86–93.
- 18 Flynn L, Semple JL, Woodhouse KA. Decellularized placental matrices for adipose tissue engineering. *J Biomed Mater Res A* 2006;79A:359–369.
- 19 Bourin P, Bunnell BA, Casteilla L et al. Stromal cells from the adipose tissue-derived stromal vascular fraction and culture expanded adipose tissue-derived stromal/stem cells: A joint statement of the International Federation for Adipose Therapeutics and Science (IFATS) and the International Society for Cellular Therapy (ISCT). *Cytotherapy* 2013;15:641–648.
- 20 Pochampally R. Colony forming unit assays for MSCs. In: Prockop DJ, Phinney DG, Bunnell BA, eds. *Mesenchymal Stem Cells: Methods and Protocols Methods*. Vol 449. In: Walker JM, ed. *Methods in Molecular Biology*. Totowa, NJ: Humana Press, 2008:83–91.
- 21 Bustin SA, Benes V, Garson JA et al. The MIQE guidelines: Minimum information for publication of quantitative real-time PCR experiments. *Clin Chem* 2009;55:611–622.
- 22 Pfaffl MW. A new mathematical model for relative quantification in real-time RT-PCR. *Nucleic Acids Res* 2001;29:2002–2007.
- 23 Sinha A, Ignatchenko V, Ignatchenko A et al. In-depth proteomic analyses of ovarian cancer cell line exosomes reveals differential enrichment of functional categories compared to the NCI 60 proteome. *Biochem Biophys Res Commun* 2014;445:694–701.
- 24 Cox J, Neuhauser N, Michalski A et al. Andromeda: A peptide search engine integrated into the MaxQuant environment. *J Proteome Res* 2011;10:1794–1805.
- 25 Cox J, Hein MY, Lubner CA et al. Accurate proteome-wide label-free quantification by delayed normalization and maximal peptide ratio extraction, termed MaxLFQ. *Mol Cell Proteomics* 2014;13:2513–2526.
- 26 Peterson AC, Russell JD, Bailey DJ et al. Parallel reaction monitoring for high resolution and high mass accuracy quantitative, targeted proteomics. *Mol Cell Proteomics* 2012;11:1475–1488.
- 27 Carmeliet P. Mechanisms of angiogenesis and arteriogenesis. *Nat Med* 2000;6:389–395.
- 28 Durr E, Yu J, Krasinska KM et al. Direct proteomic mapping of the lung microvascular endothelial cell surface in vivo and in cell culture. *Nat Biotechnol* 2004;22:985–992.
- 29 Shojaei S, Tafazzoli-Shahdpoor M, Shokrgozar MA et al. Effects of mechanical and chemical stimuli on differentiation of human adipose-derived stem cells into endothelial cells. *Int J Artif Organs* 2013;36:663–673.
- 30 Chi JT, Chang HY, Haraldsen G et al. Endothelial cell diversity revealed by global expression profiling. *Proc Natl Acad Sci U S A* 2003;100:10623–10628.
- 31 Mitchell JB, McIntosh K, Zvonc S et al. Immunophenotype of human adipose-derived cells: Temporal changes in stromal-associated and stem cell-associated markers. *STEM CELLS* 2006;24:376–385.
- 32 Delia D, Lampugnani MG, Resnati M et al. CD34 expression is regulated reciprocally with adhesion molecules in vascular endothelial cells in vitro. *Blood* 1993;81:1001–1008.
- 33 Vogel C, Marcotte EM. Insights into the regulation of protein abundance from proteomic and transcriptomic analyses. *Nat Rev Genet* 2012;13:227–232.
- 34 Culmes M, Eckstein HH, Burgkart R et al. Endothelial differentiation of adipose-derived mesenchymal stem cells is improved by epigenetic modifying drug BIX-01294. *Eur J Cell Biol* 2013;92:70–79.



See [www.StemCellsTM.com](http://www.StemCellsTM.com) for supporting information available online.